REPORT DOCUMENTATION PAGE

1a. REPORT SECURITY CLASSIFICATION UNCLASSIFIED	1b. RESTRICTIVE MARKINGS
2a. SECURITY CLASSIFICATION AUTHORITY N/A SINCE UNCLASSIFIED	3 DISTRIBUTION/AVAILABILITY OF REPORT Approved for public release; distribution is unlimited.
2b. DECLASSIFICATION/DOWNGRADING SCHEDULE N/A SINCE UNCLASSIFIED	
4. PERFORMING ORGANIZATION REPORT NUMBER(S) JSR-84-105	5. MONITORING ORGANIZATION REPORT NUMBER(S) Defense Advanced Research Projects Agency
6a. NAME OF PERFORMING ORGANIZATION The MITRE Corporation JASON Program Office 6b OFFICE SYMBOL (If applicable)	7a. NAME OF MONITORING ORGANIZATION Defense Advanced Research Projects Agency
6c. ADDRESS (City, State, and ZIP Code) 7525 Colshire Drive McLean, VA 22102	7b. ADDRESS (City, State, and ZIP Code) 1400 Wilson Boulevard Arlington, VA 22209
8a. NAME OF FUNDING/SPONSORING ORGANIZATION 8b. OFFICE SYMBOL (If applicable)	9. PROCUREMENT INSTRUMENT IDENTIFICATION NUMBER F19628-86-C-0001
8c. ADDRESS (City, State, and ZIP Code)	10. SOURCE OF FUNDING NUMBERS PROGRAM ELEMENT NO. / PROJECT NO. / TASK NO. / WORK UNIT ACCESSION NO.
11. TITLE (Include Security Classification) Neutrino Detection Primer	
12. PERSONAL AUTHOR(S) C. Callan, F. Dyson, S. Treiman	
13a. TYPE OF REPORT Technical 13b. TIME COVERED FROM _____ TO _____	14. DATE OF REPORT (Year, Month, Day) 870623 15. PAGE COUNT 90
16. SUPPLEMENTARY NOTATION	

17. COSATI CODES			18. SUBJECT TERMS (Continue on reverse if necessary and identify by block number)
FIELD	GROUP	SUB-GROUP	

19. ABSTRACT (Continue on reverse if necessary and identify by block number)

This report is intended to provide for non-expert readers a survey of natural and man-made neutrino sources and a critical review of various methods which have been proposed for their detection. Detection methods may be divided into two classes, those which have very modest performance and might actually work, and those which promise spectacular performance but violate the laws of physics. Emphasis in this report is on the second class of methods. The purpose is not to describe in detail what is possible, but to establish firm limits beyond which all schemes for detection capability are impossible. The last two sections of the report are for advanced students only and should be skipped by the non-expert. They provide precise mathematical statements and proofs of the limits which the laws of physics impose upon neutrino cross-sections. The limits are neither simple nor obvious. Consequently, it may be useful to have their technical justification here put on record.

20. DISTRIBUTION/AVAILABILITY OF ABSTRACT ☐ UNCLASSIFIED/UNLIMITED ☒ SAME AS RPT. ☐ DTIC USERS	21. ABSTRACT SECURITY CLASSIFICATION UNCLASSIFIED
22a. NAME OF RESPONSIBLE INDIVIDUAL	22b. TELEPHONE (Include Area Code) / 22c. OFFICE SYMBOL

DD FORM 1473, 84 MAR 83 APR edition may be used until exhausted. All other editions are obsolete.

Neutrino Detection Primer

MITRE

Neutrino Detection Primer

C. Callan
F. Dyson
S. Treiman

March 1988

JSR-84-105

JASON
The MITRE Corporation
7525 Colshire Drive
McLean, Virginia 22102-3481

ABSTRACT

This report is intended to provide for non-expert readers a survey of natural and man-made neutrino sources and a critical review of various methods which have been proposed for their detection. Detection methods may be divided into two classes, those which have very modest performance and might actually work, and those which promise spectacular performance but violate the laws of physics. Emphasis in this report is on the second class of methods. The purpose is not to describe in detail what is possible, but to establish firm limits beyond which all schemes for detection capability are impossible. The last two sections of the report are for advanced students only and should be skipped by the non-expert. They provide precise mathematical statements and proofs of the limits which the laws of physics impose upon neutrino cross-sections. The limits are neither simple nor obvious. Consequently, it may be useful to have their technical justification here put on record.

TABLE OF CONTENTS

LIST OF ILLUSTRATIONS

1.0 SURVEY OF SOURCES AND DETECTION METHODS

1.1 Sources

The world is awash in a flood of neutrinos.* They arise from a variety of origins, steady and episodic, natural and man-made. It would be of great scientific, and potentially of military and industrial importance, if more sensitive means than are now available could be devised for detection of neutrinos. There is a substantial community of scientific workers who are constantly on the lookout both for refinements in existing techniques and for breakthroughs. The discovery some years ago of "neutral current" interactions led a number of people to contemplate a new class of schemes based on macroscopically "coherent" detection. "Coherent" here means that the atoms in a detector work together to produce a result larger than the mere addition of the effects that would be produced by the individual atoms. Subsequent analysis, however, has shown that the anticipated sensitivities were in the main vastly overestimated. On the basis of all that can presently be foreseen, the best bet still is to work at steady improvement of macroscopically incoherent neutrino detection. "Incoherent" means that the atoms in the detector work

---

* The word neutrino is used generically in the text to denote antineutrino ($\bar{\nu}$) as well as neutrino proper (ν).

independently to produce a result which is just the sum of their individual contributions.

The most spectacular of the natural sources of neutrinos (and of much else) was the big bang and its early aftermath (the first second or so). According to standard theory, relic neutrinos left over from those early times are still around in large numbers, with isotropic flux, equal for ν and $\bar{\nu}$, of about $10^{12}/cm^2$-sec. The energies, $\sim 10^{-4}$ ev, are very tiny. Nobody has the faintest idea how to build a detector that would be sensitive to these cosmic background neutrinos. Our own sun is a (presumably steady) source of ν's, ranging in energy up to about 10 Mev. The net flux at the earth is predicted to be $\sim 6 \times 10^{10}/cm^2$-sec. The celebrated, long-running solar neutrino experiment of Davis[2] is sensitive only to the rather small fraction of ν's with energies above $\sim$ 1 Mev. From time to time supernova explosions must inundate the earth with fraction-of-a-second bursts of neutrinos peaked in the 10 Mev energy region. For "nearby" events (within our own Galaxy) one expects the onslaught to come to as much as $10^{12}/cm^2$ at the earth. In addition, the accumulated output of all supernovae over all past time should add up to a steady isotropic background of neutrinos, peaked in energy at a few Mev (remember the red shift), with isotropic flux of about $5 \times 10^3/cm^2$-sec, equal for ν and $\bar{\nu}$. The earth itself is a rather

abundant supplier of $\bar{\nu}$'s , produced in radioactive decay processes within the earth's crust. Such crustal radioactivity is thought to be the major source of heat energy generated in the earth. The by-product $\bar{\nu}$'s span an energy range up to a few Mev, with net flux at the earth's surface of about $10^7/cm^2$-sec .

Figure 1-1 is taken from Krauss, et al.[1] It shows the steady-state flux spectrum of ν and $\bar{\nu}$ at the earth's surface taking into account the sources noted above. Clearly, there are great scientific issues at stake in attempts to detect these neutrinos: early cosmology, solar burning, supernova physics, terrestrial geology, and--above all--the unexpected. What has in fact been detected so far in the Davis experiment[2], is a rather limited number of solar neutrino events, with the tantalizing finding that the rate is smaller than expected by a factor of about 3, at a 3 standard deviation level.

Man-made sources include, e.g., the Savannah River 1800 MW reactor. It corresponds to a 10^{10} curie source of $\bar{\nu}$'s , i.e., it produces about 3×10^{20} $\bar{\nu}$'s every operating second, giving a flux of about $2.5 \times 10^{13}/cm^2$-sec at a distance of 10 meters. A 150 kiloton nuclear explosion generates about 2×10^{25} $\bar{\nu}$'s , in a pulse extending over minutes. One can clearly imagine security and treaty verification reasons why it would be of the greatest importance to be able to monitor at a distance the $\bar{\nu}$'s generated in reactors or

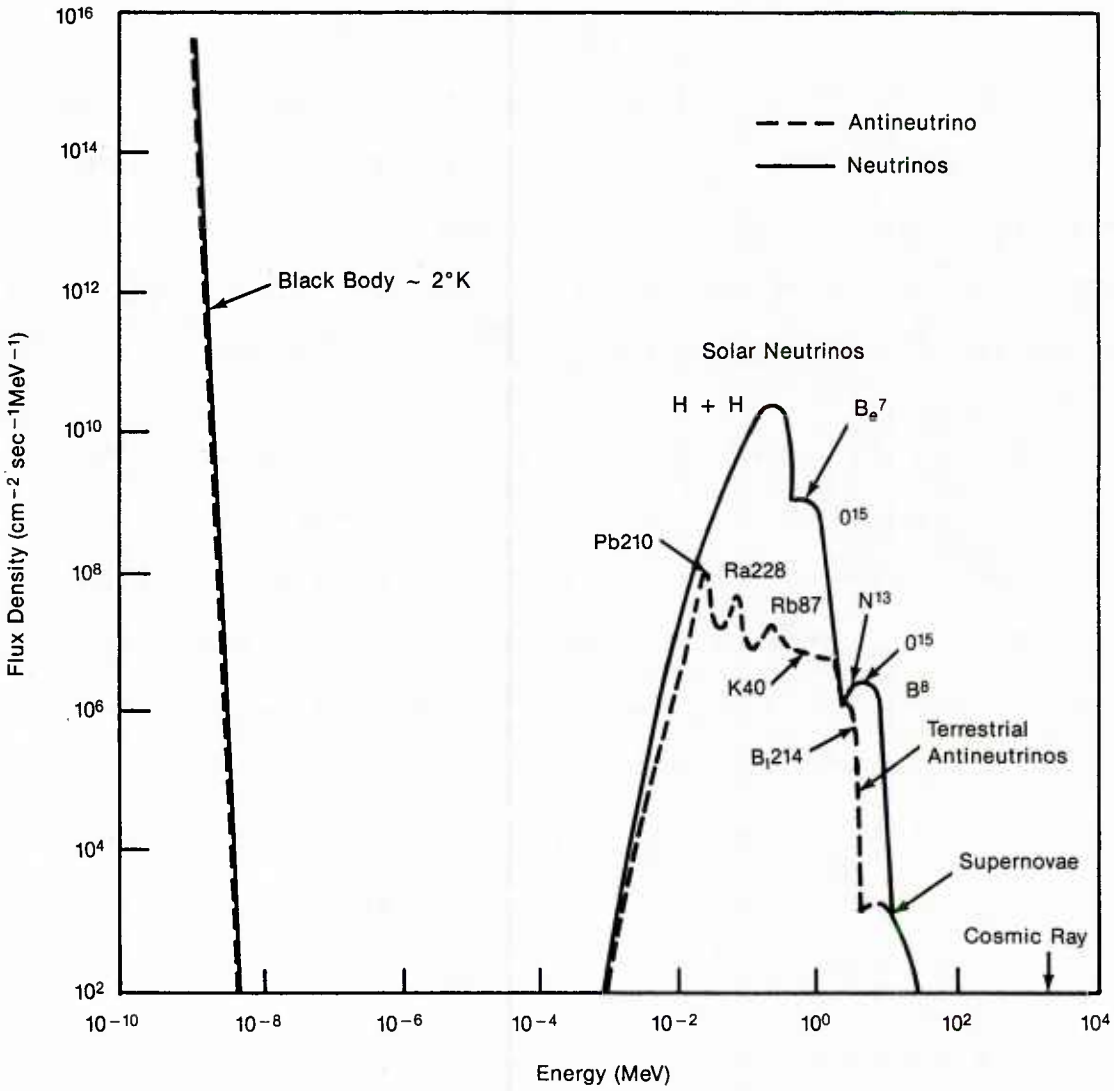

Figure 1-1. The steady-state flux spectrum of ν and $\bar{\nu}$ at the earth's surface (figure taken from Reference 1).

explosions. Neutrinos are also manufactured in high energy particle accelerators. They arise as decay products of pions, K-mesons, and other unstable particles produced in the primary collisions of high energy protons incident on target nuclei. Neutrino energies ranging up to several hundred billions of electron volts have been achieved, with up to 10^{13} neutrinos produced in a short burst, several bursts per minute. The far-out possibility of using ultra-high-energy neutrinos to probe beneath the earth's surface for oil and more general geological enlightenment has been canvassed by several high energy physicists. What this would involve is a steerable, focussed beam of neutrinos produced by a 10 trillion volt accelerator, along with sensitive detectors on the earth's surface capable of picking up tiny acoustic signals generated as the byproduct of energy deposited in neutrino collisions beneath the surface. Still others, from time to time, have contemplated the use of neutrino beams for long range communication through intervening earth and water.

For imagined applications of the above sorts, neutrinos have the great advantage that they interact weakly with matter, so can easily pass through vast thicknesses of matter without absorption or deflection. For imagined applications of the above sorts, neutrinos have the great disadvantage that they interact weakly with matter, hence do not register easily in neutrino detectors. In all neutrino detec-

tors so far employed, the neutrinos interact incoherently with the individual target atoms in the detector. By one means or another, one looks for signals that a neutrino has collided with an individual target atom. For neutrinos in the Mev region, the typical reactions are of the 2-body → 2-body type:

$$\nu + (A,Z) \rightarrow e^- + (A,Z+1) \tag{1.1}$$

"charged current" reactions

$$\bar{\nu} + (A,Z) \rightarrow e^+ + (A,Z-1) \tag{1.2}$$

and

$$\nu + (A,Z) \rightarrow \nu + (A,Z) \tag{1.3}$$

"neutral current" reactions

$$\bar{\nu} + (A,Z) \rightarrow \bar{\nu} + (A,Z) \tag{1.4}$$

Here (A,Z) denotes a nucleus with Z protons, A-Z neutrons. The strength of any particular reaction depends on the nuclear states involved and on the energy of the neutrino. It is summarized by a cross section $\sigma(E)$, where E is the neutrino energy. If F is the incident neutrino flux, N the number of target atoms irradiated, $\sigma(E)$ the relevant cross section, then the rate R of events of a

given type is

$$R = F \cdot N \cdot \sigma(E) \tag{1.5}$$

From somewhat above threshold on up to several tens of Mev, the cross sections grow quadratically with energy.

$$\sigma = \alpha\left(\frac{E}{\text{Mev}}\right)^2 \times 10^{-44}\text{cm}^2 , \tag{1.6}$$

where the parameter α can range from very small compared to unity to one or two orders of magnitude larger than unity, depending on the nuclear states involved. Even in the most favorable cases, however, the cross sections are very tiny, the detector event rates correspondingly very small. For example, in the Davis solar neutrino experiment[2], one looks radiochemically for the Ar^{37} atoms produced in the reaction

$$\nu + Cl^{37} \rightarrow e^- + Ar^{37} . \tag{1.7}$$

It takes a 400,000 liter tank of C_2Cl_4 to yield one Ar^{37} atom every two days or so!

It is the elastic neutral current reactions (elastic means that

the final and initial nuclear states are the same) that have the most favorable cross sections. This is so because the neutrons and protons in the nucleus contribute coherently for this case (it happens that the neutrons dominate over the protons). Note that we are here speaking of "microscopic coherence," the coherence of scattering by the constituent particles within a single atom. This is a very different thing from the "macroscopic coherence" which we mentioned earlier, the coherence of scattering by a huge number of atoms within a macroscopic detector. Microscopic coherence is easy to find in nature. It is macroscopic coherence that is difficult to arrange, at least in the case of neutrino interactions. The cross section is given, approximately, by

$$\sigma \approx \frac{G^2}{4\pi} (A-Z)^2 E^2 = 4 \times 10^{-45} (A-Z)^2 \left(\frac{E}{\text{Mev}}\right)^2 \text{cm}^2 , \qquad (1.8)$$

where $G = 10^{-49}$ erg-cm^3 is the so-called weak coupling constant. Coherence of the neutrons is reflected in the fact that the neutron number A-Z appears squared in σ . That neutrino interactions are weak is reflected in the fact that G is so tiny (and it contributes in the square). Elastic neutrino processes, especially in heavy nuclei (so, large A-Z), may have the most favorable of cross sections. For detection purposes, however, there is the disadvantage that the final and initial nuclear states are identical, so one

cannot recognize that an event has occurred on the basis of identifying a distinctive reaction product. Moreover, for neutrinos in the Mev range, the recoil nucleus carries little energy (at most a few hundred ev), not enough to produce discernible tracks.

For neutrinos in the multi-Gev range, neutrino collision processes cover a much wider range of possibilities. Many different final state channels are possible--states containing various multiplicities of pions, kaons, and other reaction products, along with the debris of the target nucleus. Cross sections for individual reactions tend to decrease with energy, but the total cross section, summed over all channels, again grows quadratically with neutrino energy. For neutrinos on a proton target the cross section is roughly $\sigma = 10^{-38}$ cm^2 at E = 1 Gev . In the many-Gev range the cross sections are becoming substantial (though still small compared to proton-proton collision cross sections) and neutrino reaction studies are indeed a major activity at several of the large accelerator centers.

1.2 Detectors

We are concerned in this Primer with detection of neutrinos in the Mev range. This is the range of energies relevant to neutrinos produced in reactors, bombs, and the sun. Detection in the Mev range

is enormously more difficult than in the Gev range, not only because the cross-sections are a million times smaller, but also because the effects produced by a single neutrino interaction in the Mev range are smaller and less easily distinguished from background.

It is convenient to begin our survey of real and hypothetical neutrino detectors by dividing them into four classes according to the various principles underlying their operation. The four classes are (1) Coherent Linear, (2) Coherent Quadratic, (3) Incoherent Radiochemical, and (4) Incoherent Physics. The coherent classes are those which attempt to take advantage of cooperative effects of the atoms throughout the volume of a detector. The incoherent classes are those which look for effects of neutrinos interacting with atoms one at a time. Coherent detectors offer the hope of spectacularly better performance if they can be made to work at all. Incoherent detectors are known to work but have very modest performance. The main result of our investigations is to demonstrate that coherent detectors do not work. The superior performance that they promise is illusory. All real detectors are limited to the low counting rates characteristic of incoherent detection.

The reason for the modest performance of incoherent detectors is that their rate of detection is proportional to NG^2, where N is the number of atoms in the detector and G is the weak coupling-constant

which appears in the single-atom cross-section (1.8). In a macroscopic detector, N will be a large number, of the order of 10^{29} per ton of mass, while G is exceedingly small. The two types of coherent detector attempt to escape from the NG^2 law in different ways. The coherent linear class tries to detect directly a physical quantity that is linear in the weak interaction. The performance of a coherent linear detector will thus be proportional to NG. The coherent quadratic class tries to detect effects that are coherent over the detector in cross-sections that are quadratic in the weak interaction. The performance of a coherent quadratic detector is proportional to N^pG^2, with a power p greater than 1. Hypothetical detectors have been discussed with p = 4/3, p = 5/3 and p = 2.

Coherent linear detectors are described in Sections 3 and 4 of this Primer. Coherent quadratic detectors are analyzed in Sections 5 and 6. It turns out that they fail to be practical for very different reasons. Coherent linear detectors fail because their signal-to-noise ratio is proportional to (T/T_W), where T is the duration of a measurement and T_W is the "weak interaction time"

$$T_W = \frac{\hbar c}{GF} \ . \qquad (1.9)$$

Here $\hbar$ is Planck's constant, c the velocity of light, G the weak

interaction constant, and F the flux of neutrinos to be detected. It happens that T_w is an enormously long time for any reasonable value of the neutrino flux F. For example, if F is 10^{14} neutrinos per $cm^2 sec$, T_w is 10^{11} years. Coherent linear detectors would work beautifully if we could observe for a time comparable with T_w. Unfortunately, we do not live long enough to make the observation. The failure of coherent linear detectors is not a failure in principle. They fail for quantitative reasons, as explained in Section 4.

The failure of coherent quadratic detectors is of a different character. As explained in Sections 5 and 6, they fail not for quantitative reasons but because of the poor quality of all existing sources of neutrinos. Coherent quadratic detectors would work very well if we had a source of neutrinos perfectly collimated in direction and perfectly monochromatic in energy. Unfortunately, all existing or contemplated neutrino sources have a substantial spread, either in angle or energy or both. With sources which are spread in either angle or energy, coherent quadratic detectors do not have any substantial advantage over incoherent detectors.

We conclude this introductory survey with a description of the two types of incoherent detectors. Both types have been used successfully. Incoherent radiochemical detectors use chemical methods to separate and identify the radioactive atoms produced by neutrino

interactions. The prime example of a radiochemical detector is the Davis detector using the reaction (1.7). The detector consists of a large tank full of liquid C_2Cl_4. The tank with the associated detection equipment is installed in a mine deep underground to shield it from cosmic rays. The radioactive Argon 37 atoms are collected by bubbling helium gas through the liquid. The Argon atoms are carried along with the helium and are then separated from the helium in a cold trap. After several stages of separation and concentration, the argon atoms are finally put into a tiny counter where they sit until they decay. The argon decay events are recorded by the counter. Because the detection process depends on the peculiar chemical and physical properties of argon, the detector has excellent discrimination against background events produced by cosmic rays and natural radioactivity. The advantage of good discrimination is counterbalanced by two disadvantages, low sensitivity and lack of promptness. About a month elapses on the average between each neutrino interaction and its detection. The reaction (1.7) has a threshold at 0.8 Mev and so the great majority of solar neutrinos is not detected at all.

Davis and others have made plans to build alternative radiochemical detectors with lower thresholds and higher sensitivity than the chlorine-argon detector. The preferred candidate is a gallium

detector based on the reaction

$$\nu + Ga7^{1} \rightarrow e + Ge7^{1}. \qquad (1.10)$$

This has a threshold at 0.2 Mev and should detect solar neutrinos at a rate of 10 per ton per year as compared with 0.2 per ton per year for the chlorine-argon detector. Unfortunately, gallium is expensive. Because of the high cost of gallium, present plans to build a gallium detector are on a modest scale, giving overall counting-rates comparable with the Davis detector. Because of the small cross-sections for nuclear transmutation processes such as (1.7) and (1.10), all radiochemical detectors have low sensitivity.

Incoherent physical detectors are designed to detect promptly the immediate physical effects of a neutrino interaction anywhere within the volume of a detector. The first detection of neutrinos from a reactor by Reines and Cowan[4] in 1960 was done with a physical detector, a large tank of hydrocarbon liquid with instrumentation to detect the positrons and neutrons produced in the liquid by the reaction

$$\nu + P \rightarrow n + e^{+}. \qquad (1.11)$$

This detector succeeded in detecting neutrinos at a distance of 10 meters from a high-power reactor at Savannah River.

All physical detectors have the advantage over radiochemical detectors of giving prompt detection of events. They usually have also an advantage in sensitivity. Their disadvantage is their lack of discrimination against background events of all kinds.

An ideal physical detector should detect the elastic scattering of neutrinos by nuclei, since this process has a larger cross-section than the inelastic processess (1.7), (1.10) and (1.11). The elastic scattering cross-section is given by (1.6). A detector operating with this cross-section, and using a heavy element with

$$\frac{(A-Z)^2}{A} = 90 \qquad (1.12)$$

as the scatterer, will detect solar neutrinos at a rate of about 6×10^4 per ton per year. This is an ideal upper limit which will not be approached for a long time, if ever.

Drukier and Stodolsky[3] were the first to propose a physical detector in which the recoil energy of a nucleus in an elastic neutrino scattering event is detected. They call their scheme "bolometric", since it detects the total energy deposited in the

detector by a neutrino interaction. The idea is to use small (micron-sized) superconducting grains placed in a magnetic field just below the critical strength. The heat produced in a neutrino event is supposed to be able to flip the grain from the superconducting to the normal state. Such a scheme, if it could be implemented, might constitute a large advance in sensitivity. But there are many technical obstacles still to be overcome before a prototype detector could be built.

A different kind of bolometric neutrino detector, also using physical detection and working at low temperature, has been proposed by Cabrera, Krauss and Wilczek[5]. They observe that silicon has an unusually high Debye temperature. At very low temperatures this implies that a small deposition of energy produces a detectable rise in temperature. For example, a one-kilogram block of pure silicon at 10^{-3} degrees Kelvin will rise in temperature to 4×10^{-3} degrees after absorbing 100 Kev of heat energy. This is the energy carried by the electron in a typical neutrino-electron scattering event for neutrinos with less than 1 Mev of energy. The electron comes to rest in a very short distance. Its energy is mainly converted into phonons in the silicon. Ballistic phonons transport the energy promptly from the electron track to detectors on the surface of the block, and raise the temperature of the entire block for a few

milliseconds. A neutrino event could be registered by direct detection of the ballistic phonons or by measurement of the rise in temperature. The former alternative would serve to localize the event within the silicon block. One of the virtues of silicon, in addition to its small heat-capacity at low temperatures, is its ready availability in highly purified form. Radioactive impurities are a matter of great concern. How far the silicon detector scheme can be pushed may be limited by the disturbing background decay of the radioactive isotope Silicon 32, emitting electrons with energies up to 200 Kev with a half-life of 650 years.

The Cabrera proposal raises hopes that we may achieve a sensitivity substantially higher than radiochemical detectors can offer. For solar neutrinos, the Cabrera scheme gives a theoretical counting-rate of 300 per ton per year, a factor 1000 better than chlorine-argon and only a factor 200 short of the ideal upper limit. It is likely that a Cabrera detector can actually achieve its theoretical sensitivity. It is much more doubtful whether it can achieve adequate discrimination against background events. If a Cabrera detector is to be scientifically useful, it must be extraordinarily well shielded against ambient radiation, and it must be built out of materials of extraordinary chemical purity.

The development of the Cabrera neutrino-detection technology is likely to yield rich scientific dividends. It will bring important new possibilities to particle-physics and to neutrino-astronomy. However, it is important not to expect more from it than it can deliver. At the best, if the technology fulfills all our scientific hopes, the development of it will be a slow and arduous process, an unending struggle to beat down one after another of the many possible sources of spurious background events. Like the Davis chlorine-argon detector which had to contend with many of the same difficulties, the Cabrera detector will measure its progress in decades rather than in years. Like the Davis detector, the Cabrera detector will have to sit deep underground in order to be adequately shielded from cosmic-rays. It is utterly unrealistic to imagine a Cabrera detector, or any other neutrino detector of high sensitivity, operating in the exposed environment of an ocean-going ship or submarine.

Reference 6 is a review of the incoherent neutrino detectors, radiochemical and physical, which were in various stages of study and development in 1984. Since that review was written, a new and important project has been launched to build a physical detector consisting of 6500 tons of liquid argon in an underground laboratory in Italy[7]. The detector has an estimated sensitivity of 0.5 event per ton per year, far below the sensitivity of the Cabrera detector. But

argon is cheap and easy to handle in large quantities. The idea of the argon detector is to use the argon not only as the target but as the working medium of a drift chamber, exploiting the great progress that has been achieved in recent years in drifting electrons over large distances. The inelastic reaction

$$\nu + Ar^{40} \rightarrow e + K^{40} \tag{1.13}$$

and the elastic scattering reaction

$$\nu + e \rightarrow \nu + e \tag{1.14}$$

produce fast electrons which leave behind tracks of ionization-electrons in the argon. The ionization electrons are then drifted by electric fields to a distant electrode which records their positions and times of arrival. Timing and location on the electrode plane allow us to reconstruct the direction and energy of the outgoing electron in the neutrino event. The directional information is especially helpful because it is correlated with the direction of the incident neutrinos. The electrons produced in the reaction (1.13) have a broad angular distribution, while those recoiling in the reaction (1.14) are much more strongly peaked in the direction of the incident neutrino. The argon detector has the disadvantage of low

sensitivity. It can detect neutrinos only above a high threshold energy, about 5 Mev for both the reactions (1.13) and (1.14). This means that it can detect only about 12% of fission neutrinos. It has several compensating advantages. First, it gives detailed information about neutrino energies and angular distributions. Second, it has good discrimination against background. Third, it is prompt. Fourth and most important, it has sufficient scientific and political push behind it to get it built and operating within a few years.

REFERENCES FOR SECTION 1.0

1. Krauss, Glashow, Schramm, "Antineutrino Astronomy and Geophysics," Harvard Preprint, HUTP-83/A076.

2. Davis, Evans, Cleveland, Conference Proceedings "Neutrinos-78," Purdue University, 1978, ed. Earle C. Fowler.

3. Drukier, A., and Stodolsky, L., "Principles and Applications of a Neutral Current Detector for Neutrino Physics," Phys. Rev. D30, 2295 (1984).

4. Reines, F., Cowan, C., et. al., Phys. Rev. 117, 159 (1960).

5. Cabrera, Krauss, and Wilczek, Phys. Rev. Letts. 55, 25 (1985).

6. "Solar Neutrinos and Neutrino Astronomy (Homestake 1984)," AIP Conference Proceedings, No. 126, edited by M. L. Cherry, W. A. Fowler, and K. Lande (AIP, New York, 1985).

7. See ICARUS, "A Proposal for the Gran Sasso Laboratory, INFN-AE-85-7 (September 1985) CERN," Harvard, Padova, Rome, Tokyo, Wisconsin Collaboration.

2.0 SEARCH-RATE OF AN IDEAL INCOHERENT DETECTOR

Suppose that we are using a detector, with a total cross-section Σ for detecting a neutrino, to search for submarines. Each submarine is assumed to emit N neutrinos per second. Suppose that we require at least k detected neutrinos to claim detection of a submarine. Then the search-rate for detecting submarines is

$$S = \frac{N\Sigma}{2(k-1)} \cdot \tag{2.1}$$

Note that this search-rate has the dimensions of area per second. It measures the area of ocean that can be effectively searched per second. Note also that the search-rate is independent of the velocity of motion of the detector. The faster the detector moves, the narrower the strip that it can effectively search. Note finally that the smallest possible value of k is k = 2. According to (2.1), the search-rate for k = 1 is infinite, but this infinite search-rate only expresses the fact that single neutrinos will be detected most probably from submarines at very large distances. The divergence of (2.1) for k = 1 is merely a statement of Olbers' Paradox, that in an infinite uniform ocean with a finite density of submarines the flux of neutrinos will be infinite. Neutrinos detected singly at very large distances do not give any useful information. The assumption

that k = 2 can be used for effective detection is of course exceedingly optimistic. In reality the possible value of k will be determined by the background noise level of the detector.

Proof of (2.1). For a detector proceeding along a straight track with velocity V relative to a submarine and with distance b of closest approach, the expectation-value of the number of detected neutrinos will be

$$n = \frac{N\Sigma}{4\pi} \int \frac{dt}{b^2+V^2t^2} = \frac{N\Sigma}{4bV} . \tag{2.2}$$

The probability for detecting m neutrinos will be given by the Poisson distribution

$$P_m = \frac{n^m e^{-n}}{m!} . \tag{2.3}$$

The width of the strip along both sides of the track within which m neutrinos are detected is

$$W_m = 2 \int_0^\infty P_m \, db = \frac{N\Sigma}{2V} \int_0^\infty P_m \frac{dn}{n^2}$$

$$= \frac{N\Sigma}{2V} \frac{1}{m(m-1)} . \tag{2.4}$$

The search-rate for detecting at least k neutrinos is

$$S = V(W_k + W_{k+1} + \text{---}) \ . \qquad (2.5)$$

Equations (2.4) and (2.5) together imply (2.1).

Numerical values. An ideal incoherent detector is an apparatus which detects infallibly every neutrino which impacts the theoretical cross-section

$$\Sigma = 2.4 \cdot 10^{-19} \left(\frac{(A-Z)^2}{A}\right) \left(\frac{E}{\text{Mev}}\right)^2 \left(\frac{W}{\text{Ton}}\right) \text{meter}^2 \qquad (2.6)$$

of the detector, and is untroubled by background effects. In (2.6), A and Z are the mass and charge numbers of the active ingredient of the detector, E is the neutrino energy, and W is the detector mass. The cross-section (2.6) is calculated for elastic neutrino scattering. All other neutrino interactions have substantially smaller cross-sections according to the presently accepted theory of weak interactions. The ideal incoherent detector represents an upper limit of performance which cannot, to the best of our knowledge, be surpassed.

Since all terrestrial matter has

$$\frac{(A-Z)^2}{A} < 90 \ , \tag{2.7}$$

and the neutrinos from a submarine reactor have a continuous energy-spectrum with

$$\langle E^2 \rangle = 2(\text{Mev})^2, \tag{2.8}$$

the cross-section (2.6) is at most

$$\Sigma = 4.3 \cdot 10^{-17} \ W \ (\text{meter}^2/\text{ton}). \tag{2.9}$$

The output of neutrinos from a fission reactor of power P (thermal) is

$$N = 5 \cdot 10^{17} \ P \text{ per megawatt second} \ . \tag{2.10}$$

Putting together (2.1), (2.9), and (2.10), we find the search-rate

$$S = \frac{PW}{k-1} \ , \tag{2.11}$$

with S measured in square kilometers per day, P in megawatts and W in tons. In the most optimistic case k = 2, we have in these units,

$$S = PW \ . \tag{2.12}$$

Reasonable upper-limit values for P and W are

$$P = 100 \text{ Megawatts}, \ W = 100 \text{ tons} \ . \tag{2.13}$$

Then (2.12) gives

$$S = 10^4 \ (\text{Km}^2/\text{day}) \ . \tag{2.14}$$

This is a performance comparable with a good sonar system under favorable conditions. So we have reached the conclusion that the theoretical upper limit of performance of an ideal incoherent neutrino detector is about the same as the performance of a good sonar.

This conclusion should not be misinterpreted. It does not mean that any real neutrino detector is likely to come close to achieving a search-rate of 10^4 Km^2 per day. It means only that there is no possibility that any real neutrino detector can do substantially

better than this. In reality, any practical neutrino detector will need many more than two neutrino events in order to locate a submarine. It must detect neutrinos against a variety of natural and self-generated backgrounds. For neutrino detectors as for sonars, the limits to the performance of any practical system will be set by background levels rather than by the ideal sensitivity of the instruments.

If we are detecting a nuclear explosion rather than a reactor, the formula analogous to (2.1) is

$$U = \frac{N\Sigma}{4(k-1)} . \qquad (2.15)$$

Here U is the area within which at least k neutrinos are detected, and N is now the total number of neutrinos emitted in the explosion. The equation analogous to (2.11) is

$$U = 22 \frac{YW}{k-1} , \qquad (2.16)$$

with the area U measured in square kilometers, the fission yield Y of the explosion measured in kilotons, and the active mass W of the detector measured in tons. Again, for any reasonable values of W and k, the performance of an ideal neutrino detector compares unfavorably with the performance of a seismic detector.

3.0 HISTORY OF PROPOSALS FOR COHERENT DETECTION

JASON became involved with the problem of neutrino detection as a result of a proposal submitted to DARPA by the Raytheon Corporation in 1984. We continued to be involved in 1985 as a result of a proposal to OPNAV-095 by Professor Joseph Weber of the University of Maryland. We reviewed both proposals for their respective sponsors and advised against their funding. As a response to these contentious proceedings, DARPA asked us to write a general assessment of the state-of-the-art of neutrino detection, to explain in general terms why the claims of Raytheon and Joseph Weber could not be correct. The present Primer is intended to provide such an assessment.

Both the Raytheon and the Weber proposals were for coherent neutrino detectors. The Raytheon proposal was a coherent linear scheme, the Weber proposal was coherent quadratic, in the terminology of Section 1. Our official reply to the Raytheon proposal is contained in JASON document JSN-84-1000, submitted to DARPA in August 1984. Our reply to the Weber proposal is contained in document JSR-85-210, submitted to OPNAV-095 in July 1985. Our judgment was that both proposals were flawed by gross errors in theoretical analysis.

The Raytheon proposal came to us in several versions and included several different detection schemes. Part of it was unobjectionable, being merely an implementation of the Drukier-Stodolsky scheme for incoherent bolometric detection as described in Section 1. The novel part of the Raytheon proposal was concerned with coherent detection, using a super-sensitive magnetometer to measure the magnetization induced in a sample of magnetic material by the coherent coupling between the material and a beam of neutrinos. After investigating this mode of coherent detection in detail, we concluded that it is unworkable. The details of our analysis of it are explained in Section 4. Coherent magnetic detection is an example of a phenomenon which occurs frequently in the history of science: a clever and beautiful idea killed by stubborn facts.

The Weber proposal promised even more spectacular results than the Raytheon proposal. Weber claimed that by using a perfect crystal of sapphire as a coherent quadratic detector, he could obtain detectable signals from the neutrinos emitted by a sample of radioactive tritium in the laboratory. Moreover, he claimed to have actually carried out the experiment and obtained positive results. He even claimed to be able to block the neutrino beam by interposing a second sapphire crystal between the tritium source and the detector crystal. He observed the detector signal going up and down as the

interposed crystal was moved out and in. These experimental results, with a theoretical analysis to support them, were announced in a published paper[1]. If one believed Weber's claims, the consequences would be startling. The cross-sections implied by his tritium results were about 10^{20} times larger than the cross-sections predicted by orthodox physical theory. If such large cross-sections were real, it would be an easy matter to detect neutrinos emitted by submarine reactors at distances of hundreds of kilometers.

Weber's claims naturally caused concern among responsible officials in the Navy. The officials, quite rightly, took these claims seriously. They saw one distinguished professor of physics with a published paper making these claims, and a number of other distinguished professors of physics saying in private that the claims were nonsense. How could the Navy tell who was right? If it should happen that Weber was right, it would be a matter of life and death for the submarines. So JASON was asked to study the question thoroughly and dispassionately. It was not enough to state our opinion that Weber's results were incredible. One Navy official said to us: "Didn't Lord Rutherford say that the idea of practical use of nuclear energy was moonshine? And are you JASON professors smarter than Rutherford?" To justify our belief that Weber was wrong, we had to go back to fundamentals and work through the theory of the

interaction of neutrinos with crystals from the beginning. We had to establish firm mathematical upper limits to the possible magnitude of neutrino cross-sections. The results of our investigations are recorded in Sections 5 through 8 of this Primer.

After a year's work, our conclusion is unequivocal that Weber is wrong. Weber claims that his sapphire crystal is a coherent quadratic detector with N atoms giving neutrino cross-sections proportional to N^2G^2. Furthermore, he observed a force produced by the neutrinos interacting with his crystal. This means that his detector measures a transport cross-section, a cross-section for transferring momentum between the neutrino and the crystal. We studied the theory of coherent quadratic detectors in two ways. First we made a straightforward calculation of the effects of coherent Bragg reflection on neutrino interaction with crystals. This work is summarized in Section 5. Second, we made a major effort to prove general and rigorous theorems setting upper bounds to neutrino cross-sections. The theorems and proofs are displayed in Sections 7 and 8. The main practical consequence of this work is that we can say with mathematical certainty that coherent quadratic cross-sections of the magnitude claimed by Weber do not exist. For any source of neutrinos with a wide energy-spectrum, such as a tritium source or a nuclear reactor, the possible magnitude of a transport cross-section in a

detector with N atoms is bounded by NG^2. The force exerted by neutrinos on a crystal in any experimental situation similar to Weber's will be far too small to be observed.

REFERENCE FOR SECTION 3.0

1. J. Weber, Phys. Rev. C31, (April 1985).

4.0 COHERENT DETECTION BY MEASUREMENT OF TORQUE

Neutrino cross sections are small because they are proportional to the square of the small coupling constant G. With the discovery of neutral current interactions in the 1970's, one was led for a time to the hope that observable effects to first order in G could be produced in macroscopic detectors. The idea is this: with neutral current interactions one has the possibility of forward elastic scattering, coherent over all the target particles in the detector. One can then characterize the passage of a neutrino beam through matter by an index of refraction n different from unity, where n - 1 is linear in G and in the number density of target particles. A neutrino beam carries momentum. For $n \neq 1$ one expects refraction of the beam in the passage through a piece of matter, hence momentum transfer, hence a force exerted on the matter. The early treatments of this phenomenon claimed forces linear in n-1, hence in G. Subsequent analysis, however, has revealed that the first order effects in fact cancel leaving a force which is quadratic in G and hopelessly small.

Neutrinos can also exert a coherent torque on (i.e., transfer angular momentum to) the spinning electrons of a polarized medium. Early and late analyses confirm that this torque <u>is</u> linear in G. With $\vec{S}$ the total spin angular momentum of a body (a ferromagnet,

say), $\vec{F}$ the neutrino flux, $\hbar$ the reduced Planck constant, c the speed of light, one has for the torque on the body

$$\vec{\tau} = \frac{\sqrt{2}\ G}{\hbar c} \vec{S} \times \vec{F} \qquad (4.1)$$

Although first order in G, this is nevertheless a very tiny torque, beyond foreseeable mechanical detection by many orders of magnitude.

The interaction of neutrinos and electron spins, described mechanically by the above torque, may also be pictured in terms of an equivalent magnetic interaction: namely, the electron responds as if subjected to an external magnetic field

$$\vec{H} = \frac{2\sqrt{2}\ Gm}{e\hbar} \vec{F}\ , \qquad (4.2)$$

where m is the mass, e the charge of an electron: For a ferromagnet of permeability μ, this generates an induction field $\vec{B} = \mu\vec{H}$. As with the mechanical torque, this is much too small to be detectable by foreseeable means. To show how undetectable it is, we present here a quantitative estimate of the induction effect, assuming that the detector is of the type suggested in the 1984 Raytheon proposal.

Suppose that the neutrino source is a 10^3 MW thermal reactor. The reactor produces about 10^{21} neutrinos per second. At 10 m from the reactor, the mean neutrino density turns out to be about 10^3 per cm^3. This is also the maximum neutrino density at 10^2 km from a 1 MT explosion, assuming that the neutrinos are emitted in a 1 sec pulse. Thus it seems to us that the ability to detect neutrinos at a number density of 10^3 per cm^3 is a minimum requirement.

The Raytheon proposal is to detect the small magnetization induced in a permeable medium by the effective magnetic field due to a flux of neutrinos. Roughly speaking, that field is

$$B_{EFF} \sim G_F \rho / \mu_e \ , \tag{4.3}$$

where G_F is the weak interaction constant, ρ is the neutrino density, and μ_e is the electron magnetic moment. The total effective magnetic flux through a sample of area A, in units of the flux quantum $\Phi_o = hc/e$, is

$$\Phi/\Phi_o = B_{EFF} A/(hc/e) \sim G_F \rho \ m_e A/\hbar^2 \ . \tag{4.4}$$

Using our reference value for ρ of $10^3 cm^{-3}$ and $A \sim 1\ cm^2$, we find

$$\Phi/\Phi_o \sim 10^{-19} \quad . \tag{4.5}$$

The induced magnetic flux is $\mu\Phi$ where μ is the permeability of the magnetic material. Taking $\mu \sim 10^3$ as an upper limit on achievable permeability, we have

$$\Phi_{INDUCED} \lesssim 10^{-16}\ \Phi_o \quad . \tag{4.6}$$

According to the Raytheon proposal, current SQUIDs have an internal noise of 10^{-15} Wb/m$^2/\sqrt{\text{Hz}}$ or, if the SQUID is taken to have dimensions of order 1 cm^2, an internal flux noise of $10^{-4}\ \Phi_o/\sqrt{\text{Hz}}$. In order to detect a signal of size $10^{-16}\ \Phi_o$, an integration time of 10^{24} sec is required! Although special purpose SQUIDS can certainly be built with a better noise figure than the above, there is no hope of recovering a factor of 10^{24} .

For completeness, we will analyze the noise limits on a mechanical detection scheme, not proposed by Raytheon, which seems slightly more favorable.

The weak neutral current interaction implies that if a body of total spin angular momentum $\vec{J}$ is placed in a neutrino beam of direction $\hat{n}$ and density ρ , it experiences a torque

$$W = \left(k \frac{G_F}{\sqrt{2}} \frac{\rho}{\hbar} \hat{n}\right) \times \vec{J} \qquad (4.7)$$

where k is a constant of order 1 depending on the detailed composition of the body. For purposes of illustration, we assume that the spins are rigidly coupled to the body so that the interaction with the neutrinos produces an acceleration of the body as a whole. The maximum spin density of iron is roughly $2 \times 10^{23}\ \hbar\ (cm^{-3})$. The maximum torque on a $1\ cm^3$ sample in our reference neutrino beam is therefore

$$W_{max} \sim G_F \cdot \frac{\rho}{h} \cdot (2 \times 10^{23}\ \hbar/cm^3) \sim 2 \times 10^{-23}\ erg\ . \qquad (4.8)$$

The corresponding maximum angular acceleration of the body will be

$$\alpha_{max} \sim .4 \times 10^{-23}\ sec^{-2} \qquad (4.9)$$

(assuming a moment of inertia equal to $5\ gm\ cm^2$) and the maximum linear acceleration of a point on the body will be

$$a_{max} \sim .4 \times 10^{-23}\ cm\text{-}sec^{-2} \qquad (4.10)$$

(assuming a maximum linear dimension of 1 cm). Note that if L is the

linear dimension of the body, the torque scales as L^3 and the moment of inertia scales as L^5, so that α_{max} and a_{max} scale as L^{-2} and L^{-1} respectively. There is an advantage to using <u>small</u> detectors in this scheme, but a gain of a few powers of ten will not, as we shall see, solve our problems.

Is there any hope of measuring such a tiny macroscopic acceleration? Virtually the same problem arises in the study of mechanical gravity-wave antennas and in the new field of attempts to measure the hypothetical axion-mediated force between macroscopic bodies. We have consulted a recent (excellent!) PhD thesis on this subject by J. Moody to learn the current state-of-the-art. The main problem is thermal noise, whose level is given by

$$a_{therm} = \left(\frac{4\ kT}{m\tau\tau^*} \right)^{1/2} \qquad (4.11)$$

where τ is the observation time, τ^* is the system relaxation time and m is its mass. We will take T = 1 mK and m = 1g. Because of the nature of the signals we wish to detect, we must take $\tau \sim 1$ sec (a narrower bandwidth would be better, but we don't see how to get it!). Nobody knows how high τ^* can go in a low temperature mechanical system constructed out of perfect crystals: $\tau^* = 10^8$ sec is certainly possible, and optimistic estimates (taken from Moody's

thesis) suggest that $\tau^* = 10^{13}$ sec might be obtainable with much hard work. Taking the optimistic value of $\tau^* = 10^{13}$s , we get a thermal noise limit of

$$a_{therm} \sim 10^{-16} \text{ cm/s}^2 . \qquad (4.12)$$

This is seven orders of magnitude greater than the signal level produced by our reference neutrino source, from which we conclude that coherent neutrino detection by mechanical means is hopeless.

The Moody thesis covers other detection schemes than the one discussed above, but the conclusion is the same. As a reading of the Moody thesis will indicate, there is strong physics interest in developing schemes for measuring accelerations in the 10^{-22} cm/s^2 area, and perhaps DARPA should keep an eye on the field, against the day when a bright idea will make it possible. That day will certainly not dawn for many years.

REFERENCE FOR SECTION 4.0

1. Moody, J. E., "Axion Forces, Gravity Experiments and T-Violation," Princeton Ph.D. Thesis (1984).

5.0 COHERENT DETECTION BY BRAGG REFLECTION

The purpose of this section is to obtain a qualitative understanding of coherent effects in the scattering of neutrinos by crystals. These are the effects which are supposed to be exploited in the Weber experiment (described in Section 3) and in other schemes for coherent quadratic detection. To simplify the discussion, we ignore in this section the internal dynamics of the crystal. We calculate the neutrino scattering produced by a perfectly rigid crystalline lattice without internal degrees of freedom. The effects of the internal dynamics of the scatterer will be properly taken into account in the more accurate calculations of Sections 7 and 8.

We consider first the elastic scattering of a neutrino by a crystal. A neutrino of energy E and wave-vector k with

$$|k| = (E/\hbar c) \tag{5.1}$$

will be scattered by a single atom with cross-section

$$\sigma_o = AE^2 , \tag{5.2}$$

the coefficient A being of the order of magnitude

$$A \sim (G^2 / \hbar^4 c^4) \sim 10^{-44} (cm^2/MeV^2), \qquad (5.3)$$

where G is the Fermi coupling constant. The incoherent scattering from N atoms will be

$$\sigma_I = N\sigma_o = NAE^2 \quad . \qquad (5.4)$$

In principle, one might obtain a much larger cross-section by using as scatterer a perfect crystal of $N = n^3$ identical atoms in a cubic lattice. The differential cross-section for coherent scattering into the state with wave-vector p is

$$\sigma_d = (AE^2 / 4\pi) F(p - k) \quad , \qquad (5.5)$$

where F(q) is the form-factor of the lattice. F(q) is a function of the vector q having sharp maxima at the vertices of the reciprocal cubic lattice. The reciprocal lattice has spacing

$$b = (2\pi/a) \quad , \qquad (5.6)$$

where a is the lattice-spacing of the crystal. Each maximum of F(q) is a blob with a peak value

$$N^2 = n^6 \tag{5.7}$$

and a volume of the order of

$$(b/n)^3 \ . \tag{5.8}$$

The condition for a coherent Bragg reflection is that one of the blobs of the form-factor F should intersect the sphere

$$| p | = (E / \hbar c) \ . \tag{5.9}$$

When this condition is satisfied, the differential cross-section according to (5.5) is

$$\sigma_d = (AE^2N^2 / 4\pi) \ . \tag{5.10}$$

For a macroscopic crystal with $n = 10^8$, $N = 10^{24}$, and a neutrino energy E = 1 MeV, the cross-section (5.10) is

$$\sigma_d \sim 10^3 \text{ cm}^2/\text{steradian} \ . \tag{5.11}$$

The large cross-section may give a misleading impression that the scattering should be easily detectable.

In fact the experimentally relevant quantity is not the differential cross-section but the total cross-section integrated over a blob. The blob occupies a solid angle of order

$$\left(\frac{b}{n|p|} \right)^2 = \left(\frac{hc}{naE} \right)^2 \tag{5.12}$$

on the surface of the sphere (5.9), and the total coherent cross-section is therefore

$$\begin{aligned} \sigma_c &= \frac{AE^2N^2}{4\pi} \left(\frac{hc}{naE}\right)^2 \\ &= \pi N^{4/3} A(\hbar c/a)^2 \\ &= \pi N^{4/3} (G/\hbar ca)^2 \sim 10^{-49} N^{4/3} \text{ cm}^2 , \end{aligned} \tag{5.13}$$

for a crystal with lattice-spacing $a \sim 10^{-8}$ cm. This cross-section is no longer so impressively large. The ratio of coherent to incoherent scattering is by (5.4) and (5.13)

$$\begin{aligned} R = (\sigma_c/\sigma_I) &= \pi N^{1/3} (\hbar c/aE)^2 \\ &\sim \pi N^{1/3} 10^{-5} \left(\frac{\text{MeV}}{E} \right)^2 . \end{aligned} \tag{5.14}$$

This ratio could in principle be as large as 10^8 for neutrinos with energy of a few kilovolts.

However, the Bragg scattering condition can only be satisfied by neutrinos for which the sphere (5.9) comes within a distance (b/n) of some fixed reciprocal lattice-vector $\bar{q}$. That is to say, the neutrino wave-number k must satisfy

$$|k + \bar{q}| = |k| + \varepsilon, \quad |\varepsilon| < (b/n), \tag{5.15}$$

or

$$2|k|\bar{q}_{\parallel} + \bar{q}^{\,2} = 2\varepsilon|k| + \varepsilon^2, \tag{5.16}$$

where $\bar{q}_{\parallel}$ is the component of $\bar{q}$ parallel to k. Differentiating (5.16) while keeping $\bar{q}$ fixed, we find

$$\frac{d\varepsilon}{dk} = \frac{\bar{q}_{\parallel}}{|k|} = -(1-\cos\theta), \tag{5.17}$$

where θ is the scattering angle, the angle between k and p. Since ε has to lie in the range (5.15), the Bragg condition can only be satisfied for neutrinos which are monoenergetic within an accuracy

$$\Delta E = N^{-1/3}\,(hc/a)\,(1-\cos\theta)^{-1}. \tag{5.18}$$

There are now two cases to consider. If the scattering is in the forward direction with $\theta = 0$, the Bragg condition is satisfied

for all energies and the bound (5.18) imposes no restriction. So for forward scattering we have a total cross-section proportional to $N^{4/3}$ as in (5.13), without any restriction on the incident neutrino energy. This $N^{4/3}$ forward cross-section is merely the familiar diffraction peak produced when a plane wave is diffracted by an extended obstacle.

For scattering in any direction other than forward, the condition (5.18) means that cross-sections of order $N^{4/3}$ can only be obtained for neutrinos which are monoenergetic to within an accuracy of order $N^{-1/3}$. For any incident flux of neutrinos with a broad energy-spectrum, the enhancement factor $N^{1/3}$ in (5.14) is cancelled out by the factor $N^{-1/3}$ in (5.18). For broad-spectrum neutrinos such as those arising from fission-product decay in reactors, the coherent cross-section averaged over the energy-spectrum is equal to the incoherent cross-section (5.4) similarly averaged. The use of a coherent crystal scatterer gives no advantage.

The best known flux of monoenergetic neutrinos in nature comes from the reaction

$$P + e + P \rightarrow D + \nu \qquad (5.19)$$

in the sun. These so-called Pep neutrinos have energy 1.4 MeV with a thermal spread of the order of a kilovolt. According to (5.18) the

coherent scattering is only enhanced within an energy-band of the order

$$\Delta E \sim 10\ N^{-1/3}\ \text{Kilovolts}\ , \qquad (5.20)$$

and the thermal spread is far too broad for the enhancement to be significant. Other possible sources of monoenergetic neutrinos, such as the electron-capture decays of N_{13} and O_{15} produced in carbon-cycle reactions in the sun, also have energies in the MeV range and energy-spread due to thermal Doppler effect in the Kilovolt range. In all cases the enhancement given by (5.14) will be unobservable.

To conclude this discussion of elastic scattering, we may summarize it by saying that enhanced cross-sections proportional to $N^{4/3}$ can occur only under two conditions. Either the scattering is forward and transfers no momentum to the scatterer, or we are in a condition of true Bragg reflection and the neutrinos must be monoenergetic. In the first case, the scattering is unobservable because it produces no change in the state of the scatterer or of the neutrino. In the second case the scattering is unobservable because we have no adequately monoenergetic sources.

It is of some interest to generalize the foregoing discussion to elastic transmutation processes. Here "elastic" means that the interaction does not change the internal state of the scatterer,

while "transmutation" means that the interaction changes the internal state of the scattered particle. We suppose then that an incident particle, which may or may not be a neutrino, has rest-mass M, and is transmuted by the scatterer into an outgoing particle with rest-mass M'. In the case of a neutrino capture reaction such as (1.7), M is zero and M' is the rest-mass of an election.

The single-atom cross-section (5.2) then becomes

$$\sigma_o = AE^2 (v'/v). \tag{5.21}$$

where

$$v' = (\hbar c|p|/E),\ v = (\hbar c|k|/E) \tag{5.22}$$

are the velocities of the outgoing and incident particles. We assume that the scatterer absorbs no energy, so that

$$M^2c^4 + h^2c^2|k|^2 = M'^2c^4 + h^2c^2|p|^2. \tag{5.23}$$

The condition for a Bragg reflection is the same as before, only now the solid-angle (5.12) becomes

$$\left(\frac{b}{n|p|}\right)^2 = \left(\frac{hc^2}{naEv'}\right)^2, \tag{5.24}$$

and the coherent cross-section (5.13) becomes

$$\sigma_c = \pi N^{4/3} (G^2/\hbar^2 a^2 v\, v') \ . \qquad (5.25)$$

The surprising and novel feature of (5.25) is that we can in principle obtain enormous coherent cross-sections by making the velocity v' of the outgoing particle very small.

How large can the coherent cross-section become? The formula (5.25) cannot be correct all the way to v' = 0. In fact (5.25) fails when the outgoing wave-vector p is so small that the solid angle (5.24) becomes larger than unity. The maximum cross-section is obtained when $|p|$ is of the order (b/n). This means that the entire sphere

$$|k + \bar{q}| = |p| \qquad (5.26)$$

lies inside one of the blobs surrounding the reciprocal lattice-vector $\bar{q}$, and so the total scattering cross-section is just the differential cross-section multiplied by the total solid angle 4π. The total cross-section is then by (5.21)

$$\sigma_c = N^2 \sigma_o = AN^2 E^2 (v'/v) \ . \qquad (5.27)$$

Since $|p|$ is of order $n^{-1} = N^{-1/3}$, (v'/v) is also of order $N^{-1/3}$, and (5.27) gives

$$\sigma_c \sim N^{5/3} AE^2 . \qquad (5.28)$$

So we find unexpectedly that it is possible to obtain total cross-sections of order $N^{5/3}$ for transmutation processes, if the energy of the incident particle is fine-tuned to give a Bragg reflection very close to zero outgoing velocity. The existence of this artificial $N^{5/3}$ singularity for transmutation processes turned out to be the main obstacle which we had to overcome in proving theorems to set firm upper limits to cross-sections. Any theorem which says that cross-sections can at most be of order N or $N^{4/3}$ must have an escape clause to avoid the zero-outgoing-velocity singularity.

The most useful way to avoid the $N^{5/3}$ singularity is to average cross-sections over the energy E of the incident particle. Since the $N^{5/3}$ singularity occurs only for an exceedingly narrow range of energies, it will disappear from the averaged cross-sections.

In the case of a transmutation process, the condition for a Bragg reflection becomes instead of (5.15)

$$|k + \bar{q}| = |p| + \varepsilon, \ |\varepsilon| < (b/n) , \qquad (5.29)$$

When we differentiate (5.29), using the energy equation (5.23) to determine the relation between $|k|$ and $|p|$, we obtain instead of (5.18)

$$\frac{d\varepsilon}{dk} = \cos\theta - \left(\frac{v}{v'}\right) . \qquad (5.30)$$

The range of energy over which the Bragg condition can be satisfied then becomes

$$\Delta E = N^{-1/3} (h/a) \left(\frac{v\, v'}{v - v' \cos\theta}\right) . \qquad (5.31)$$

For an energy-averaged cross-section we must multiply the Bragg-reflection cross-section (5.25) by the energy-range (5.31). The result is

$$\bar{\sigma}_c = 2\pi^2 N (G^2/\hbar a^3) (v - v' \cos\theta)^{-1} . \qquad (5.32)$$

In the energy-averaged cross-section, both the factor $N^{4/3}$ and the singular factor $(v')^{-1}$ have disappeared. There is no longer a problem of an artificially enormous cross-section at small values of v'. All that is left in (5.32) is a singularity at $\theta = 0$, $v' = v$. This singularity is the familiar and physically reasonable forward peak in the elastic scattering cross-section, the same peak which appeared in (5.18). The peak in forward elastic scattering does not depend on Bragg reflection and is unaffected by averaging over the incident energy. In order to get rid of this forward peak, one must look at quantities other than total cross-sections.

An easy way to get rid of the forward elastic singularity in (5.32) is to consider the transport cross-section, conventionally defined as the integral over angle of the differential cross-section multiplied by the factor $(1 - \cos \theta)$. The $(1 - \cos \theta)$ cancels the singularity of (5.32). We thus obtain an energy-averaged transport cross-section which is uniformly finite and proportional to N. We shall prove in Sections 7 and 8 that energy-averaged transport cross-sections are rigorously bounded with a bound proportional to N. The example considered in this Section 5 shows that no stronger statement can be true. Both the energy-averaging and the $(1 - \cos \theta)$ factor are necessary in order to obtain a bound proportional to N.

Another way to get rid of the forward elastic singularity is to consider inelastic processes in which the scatterer absorbs energy from the incident particle. It is convenient to define an inelastic cross-section as the integral of a differential cross-section multiplied by the factor $(1 - (E'/E))$, where E' is the energy of the outgoing particle, E the energy of the incident particle. The inelastic cross-section then measures the rate of transfer of energy to the scatterer, just as the transport cross-section measures the rate of transfer of momentum.

6.0 THEORETICAL UPPER BOUNDS: MAIN RESULTS AND IMPLICATIONS

We are now entering the domain of rigorous mathematics. We wish to obtain reliable upper bounds for the size of cross-sections for the interaction of neutrinos with a detector containing a large number N of atoms. We are concerned with four kinds of cross-section. Differential cross-sections,

$$\sigma\ (k,k')\ d\Omega' dE', \tag{6.1}$$

for interactions in which an incident particle with wave-vector k is converted into an outgoing particle with direction in a small solid angle $d\Omega'$ and energy in a small interval dE' around the out-going wave-vector k'. Total cross-sections, obtained by integrating (6.1) over energy and angle,

$$\sigma_T(k) = \iint \sigma\ (k,k')\ d\Omega'\ dE'\ . \tag{6.2}$$

Transport cross-sections, obtained by integrating the differential cross-section with the weighting-factor $(1-\cos\theta)$,

$$\sigma_{TR}(k) = \iint \sigma\ (k,k')\ (1-\cos\theta)\ d\Omega'\ dE', \tag{6.3}$$

where θ is the angle between k and k'. Inelastic cross-sections, obtained by integrating (6.1) with the weighting factor $\left(1 - (E'/E)\right)$.

$$\sigma_{IN}(k) = \iint \sigma\,(k,k') \left(1- (E'/E)\right) d\Omega'\, dE' \,. \qquad (6.4)$$

The total cross-section is not a measurable quantity since it includes the large diffraction peak at forward angles. Forward elastic scattering has no observable effect either on the neutrino or on the scatterer. All real detectors are effectively measuring either the transport or the inelastic cross-section. The Weber detector, which is designed to detect directly the momentum transferred from neutrinos to the scatterer, is measuring the transport cross-section. Bolometric detectors are directly measuring the inelastic cross-section defined by (6.4). Radiochemical detectors are measuring the cross-section for a single reaction which is included in (6.4). The liquid-argon detector measures cross-sections for various processes which are also included in (6.4). Any detector which detects the recoil energy in neutrino scattering events is effectively measuring (6.4). Every detector, real or contemplated, measures a cross-section which is bounded either by the transport or by the inelastic cross-section.

We have seen in Section 5 that coherent effects can produce differential cross-sections of order N^2. This happened in the example of scattering of neutrinos by a rigid crystal lattice. In that example, large singularities also appeared in total and transport cross-sections. There were three distinct types of singularity.

Type A. Forward angle peak due to elastic diffraction. This produces

$$\sigma_T(k) \sim N^{4/3}, \quad \sigma_{TR}(k) \sim N \ . \tag{6.5}$$

Type B. Ordinary Bragg-reflection peak. This gives

$$\sigma_T(k) \sim \sigma_{TR}(k) \sim N^{4/3} \ . \tag{6.6}$$

Type C. Bragg-reflection peak with outgoing velocity close to zero. This gives

$$\sigma_T(k) \sim \sigma_{TR}(k) \sim N^{5/3} \ . \tag{6.7}$$

Our theorems are designed to demonstrate that all observable cross-sections are bounded by bounds of order N. The theorems must

therefore be formulated in such a way that all three types of singularity disappear. By working with σ_{TR} and σ_{IN} rather than σ_T we make the Type A singularity disappear, but types B and C still remain. To remove the Types B and C singularities, it turns out to be sufficient to deal with cross-sections averaged either over the incident energy or over the incident angle. Thus we consider the quantities

$$\mathrm{Av}_E\ \sigma_{TR}(k) = \int_0^1 \sigma_{TR}\big(k\ (xE)\big)\ dx \tag{6.8}$$

and

$$\mathrm{Av}_\Omega\ \sigma_{TR}(k) = \frac{1}{4\pi} \int \sigma_{TR}\ (k_\Omega)\ d\Omega\ , \tag{6.9}$$

where k(xE) means a wave-vector parallel to k but corresponding to a particle of energy (xE) instead of E, and k_Ω means a wave-vector with direction Ω and magnitude $|k|$. We define in the same way the averaged total and inelastic cross-sections. If a neutrino source has a finite energy band-width B with maximum energy E_M, then it will give a transport cross-section bounded by

$$(E_M/B)\ \mathrm{Av}_E\sigma_{TR}(k)\ . \tag{6.10}$$

And similarly, if a source has a finite angular size with solid-angle A, then it will give a transport cross-section bounded by

$$(4\pi/A)\ \mathrm{Av}_{\Omega}\ \sigma_{TR}(k)\ . \qquad (6.11)$$

So our bounds for (6.8) and (6.9) will give bounds for all transport cross-sections for neutrino sources which are spread over finite ranges of energy or angle.

The bounds which we have established are summarized in Table 6-1. All these bounds are best possible, as shown by the example which we studied in Section 5. The four bounds proportional to N prove that no observable neutrino cross-sections can be significantly greater than the standard incoherent atomic cross-sections. In particular, they imply that Weber's detector cannot have the performance which Weber claimed for it. And they imply that the estimates calculated in Section 2 for the search-rate of an ideal incoherent detector are equally valid for coherent detectors.

The question-mark in Table 6-1 means that we have not been able to establish the true upper bound for inelastic cross-sections at fixed energy and fixed angle. This remains a problem for the future. We conjecture that inelastic cross-sections at fixed energy and angle are bounded with a bound proportional to N, but we failed to find a proof. The calculations of Section 5 gave no information about inelastic cross-sections, since they referred only to

TABLE 6-1

THEORETICAL BOUNDS TO NEUTRINO CROSS-SECTIONS
FOR A MACROSCOPIC DETECTOR CONTAINING N ATOMS

	Total	Transport	Inelastic
Fixed Angle Fixed Energy	$N^{5/3}$	$N^{5/3}$	?
Fixed Energy Smeared Angle	$N^{4/3}$	N	N
Fixed Angle Smeared Energy	$N^{4/3}$	N	N

These powers of N multiply the standard neutrino cross-section for a single atom:

$$\sigma_o \sim \frac{G^2E^2}{\hbar^4 c^4} \sim 10^{-44} \text{ cm}^2 .$$

scattering and transmutation by a rigid lattice potential which had no internal structure to absorb energy. All the processes considered in Section 5 were elastic and gave zero contribution to the inelastic cross-section (6.4). The true upper bound for inelastic cross-sections might, so far as we know, lie anywhere in the range from N to $N^{5/3}$. Fortunately, we can prove bounds of order N for inelastic cross-sections averaged over energy or over angle, and these bounds are sufficient for application to any real detector.

7.0 THEORETICAL UPPER BOUNDS: EXACT DEFINITIONS AND THEOREMS

We wish to find firm theoretical upper bounds for the cross-sections for the interactions of neutrinos with macroscopic objects. We assume that the interaction is represented by a local coupling

$$H(r) = GJ^{\alpha}(r)\, j_{\alpha}(r) \tag{7.1}$$

between the current $J^{\alpha}(r)$ carried by the various particles in the scatterer and the current $j_{\alpha}(r)$ carried by neutrinos. G is the coupling constant of the weak interaction,

$$G = 10^{-49} \text{ erg cm}^3. \tag{7.2}$$

The weak current $j_{\alpha}(r)$ has various components, converting an incoming neutrino into an outgoing neutrino, electron or other species of lepton. We calculate cross-sections treating H(r) as small, working with first-order perturbation theory. That is to say, we are ignoring possible subsequent interactions between the outgoing lepton and the scatterer.

We calculate cross-sections for an incident neutrino with wave-vector k, energy E, and an outgoing lepton with wave-vector k', energy E'. The momentum transferred to the scatterer is $\hbar q$, where

$$q = k - k'. \tag{7.3}$$

The matrix element of $j_\alpha(r)$ for this transition is

$$\langle j_\alpha(r)\rangle = j_\alpha \exp\,(iq \cdot r), \tag{7.4}$$

where j_α is a number independent of r and q. The interaction will bring the scatterer from an initial state 0 with wave-number p_o and energy E_o to a final state f with wave-number p_f and energy E_f. Since momentum and energy are conserved,

$$-q = p_o - p_f, \tag{7.5}$$

$$E - E' = E_f - E_o. \tag{7.6}$$

The matrix element of $J^\alpha(r)$ for the transition will be

$$\langle J^\alpha(r)\rangle = (J^\alpha)_{fo} \exp\,(-iq\cdot r). \tag{7.7}$$

The matrix element $(J^\alpha)_{fo}$ will be independent of r but will depend in a complicated fashion on the internal structure of the scatterer in the initial and final states. It is important to observe that

$(J^{\alpha})_{fo}$ is also formally independent of q, although in fact q is determined by (7.5) as soon as the initial and final states o and f are specified.

Putting together (7.1) with (7.4), we have for the matrix element of H(r) in the transition

$$\langle H(r)\rangle = \langle K(r)\rangle_{fo} \exp\,(iq\cdot r), \tag{7.8}$$

$$K(r) = Gj_{\alpha}\, J^{\alpha}(r). \tag{7.9}$$

This K(r) is an operator acting upon the scatterer only, the neutrino part of the matrix element having been taken care of by (7.4). In fact K(r) is a local current operator describing the structure of the scatterer at the point r.

We wish to make a minimum of assumptions concerning the internal dynamics and structure of the scatterer. The essential requirement is that the scatterer be an extended object of finite density so that the effects of the local operator K(r) are not too highly concentrated in space. It will turn out that all we need to know about the structure of the scatterer is contained in the auto-correlation function

$$A(r,r') = \langle K(r)\, K(r') \rangle_{oo}, \tag{7.10}$$

the expectation-value in the initial state of the scatterer of the product of two local currents at r and r'. The notion that the scatterer is an extended object of finite density is expressed mathematically as follows. The autocorrelation function is a sum of two parts, one bounded and the other short-range.

$$A(r,r') = B(r,r') + S(r,r') , \tag{7.11}$$

$$|B(r,r')| < G^2\rho^2 , \tag{7.12}$$

$$\left|\int S(r,r')\, dr'\right| < G^2\rho , \tag{7.13}$$

where ρ is an upper bound to the density of particles in the scatterer. The short-range part S(r,r') will have a singularity at r = r' due to the operation of the two operators K(r) and K(r') on the same particle in the scatterer. The long-range part B(r,r') has no singularity since it arises from the operation of K(r) and K(r') on different particles. The conditions (7.12) and (7.13) express the requirement that the particles in the scatterer are nowhere concentrated more densely than ρ particles per cm^3.

The only other condition which we impose upon the scatterer is that its initial state 0 should be the ground-state. Thus

$$E_f \geq E_o \tag{7.14}$$

for every final state f. This condition is not physically realistic, since any real scatterer will be at a finite temperature. It would be possible to avoid the assumption (7.14) at the cost of some additional mathematical complication in our proofs. The practical excuse for assuming (7.14) is that the thermal energies of particles in the scatterer are very small compared with neutrino energies.

The differential cross-section for the transition from incident wave-number k to outgoing wave-number k' is

$$\sigma(k,k') = \frac{b^2}{h^2 vv'} \Sigma_f \, \delta(E_f - E_o - E + E') \left| \int dr \, < K(r) >_{fo} \exp(iq\cdot r) \right|^2 . \tag{7.15}$$

Here v,v' are the velocities of the incident and outgoing leptons,

$$\hbar v = \frac{dE}{da} = \frac{\hbar^2 c^2 a}{E} , \quad \hbar v' = \frac{dE'}{db} = \frac{\hbar^2 c^2 b}{E'} ,$$

$$a = |k| , \; b = |k'| . \tag{7.16}$$

According to (6.2), this cross-section is differential in both angle and energy of the outgoing particle. The total cross-section is obtained from (7.15) and (6.2), the transport cross-section and the inelastic cross-section from (7.15), (6.3) and (6.4).

In order to formulate our theorems, it is convenient to define a number of other weighted cross-sections with various weights. These are as follows:

$$\sigma_A(k) = \iint \sigma(k,k') \frac{|k-k'|}{|k|} \, d\Omega' dE', \tag{7.17}$$

$$\sigma_B(k) = \iint \sigma(k,k') \left[1 - \left(\frac{v'}{v}\right) \cos\theta\right] d\Omega' dE', \tag{7.18}$$

$$\sigma_F(k) = \iint \sigma(k,k') \left[1 - \frac{|k'|}{|k|} \cos\theta\right] d\Omega' dE', \tag{7.19}$$

$$\sigma_V(k) = \iint \sigma(k,k') \left(\frac{v'}{v}\right) d\Omega' dE', \tag{7.20}$$

$$\sigma_W(k) = \iint \sigma(k,k') \left(1 - \frac{E'}{E}\right) \left(\frac{v'}{v}\right) d\Omega' dE'. \tag{7.21}$$

It happens that $\sigma_F(k)$ is the quantity directly measured in a detector of Weber type which observes the force exerted on the scatterer by the neutrinos. The other four cross-sections are those which arise naturally in the proofs of our theorems. The operation of energy-averaging and angle-averaging are defined for these cross-sections as in (6.8) and (6.9). Our theorems are then:

Theorem 1. $$Av_\Omega \sigma_A(k) < N\sigma_1, \tag{7.22}$$

Theorem 2. $$Av_E \sigma_B(k) < N\sigma_2, \tag{7.23}$$

Theorem 3. $$\sigma_v(k) < N^{4/3}\,\sigma_3, \tag{7.24}$$

Theorem 4. $$\sigma_w(k) < N\sigma_4. \tag{7.25}$$

Here N is the number of atoms in the scatterer, and σ_1, σ_2, σ_3, σ_4 are microscopic cross-sections which depend on the local density and composition of the scatterer but are independent of N.

The various cross-sections are related by inequalities which are easy to verify.

$$\sigma_{IN}(k) < \sigma_F(k) < \sigma_A(k) \ . \tag{7.26}$$

$$\sigma_F(k) < \sigma_B(k) + \sigma_w(k) \ . \tag{7.27}$$

$$\sigma_T(k) < \sigma_B(k) + \sigma_v(k) \ . \tag{7.28}$$

$$\sigma_{TR}(k) < 2\sigma_B(k) \ . \tag{7.29}$$

$$\sigma_B(k) < 2\sigma_F(k) \ . \tag{7.30}$$

By virtue of these inequalities, the four theorems lead immediately to the following seven corollaries.

Corollary 1. $Av_\Omega \sigma_{TR}(k) < N\sigma_5$. (7.31)

Corollary 2. $Av_\Omega \ \sigma_{IN}(k) < N\sigma_6$. (7.32)

Corollary 3. $Av_E \sigma_{TR}(k) < N\sigma_7$. (7.33)

Corollary 4. $Av_E \sigma_{IN}(k) < N\sigma_8$. (7.34)

Corollary 5. $Av_\Omega \sigma_T(k) < N^{4/3}\sigma_9$. (7.35)

Corollary 6. $$Av_E\sigma_T(k) < N^{4/3}\sigma_{10}. \tag{7.36}$$

Corollary 7. $$\sigma_T(k) < N^{5/3}\sigma_{11}. \tag{7.37}$$

In fact, Corollary 1 follows from (7.26), (7.29), (7.30) and Theorem 1. Corollary 2 follows from (7.26) and Theorem 1. Corollary 3 follows from (7.29) and Theorem 2. Corollary 4 follows from (7.26), (7.27) and Theorems 2 and 4. Corollary 5 follows from (7.26), (7.28), (7.30) and Theorems 1 and 3. Corollary 6 follows from (7.28) and Theorems 2 and 3. Finally, Corollary 7 follows from Theorem 3 and from the fact that the differential cross-section $\sigma(k,k')$ can at most be of order N^2.

The seven Corollaries (7.31) to (7.37) provide the basis for each of the entries in the summary Table 6-1 of Section 6. All that now remains for Section 8 is to supply the proofs of the four theorems.

8.0 THEORETICAL UPPER BOUNDS: PROOFS

8.1 Proof of Theorem 1

When we substitute (7.15) into (7.17) and average over angle according to (6.9), the result is

$$Av_{\Omega}\sigma_A(k) = \iint d_3q\, dE' \left(\frac{|q|}{a}\right) F(a,b,q)\, S(a,b,q) , \tag{8.1}$$

with the factors F(a,b,q) and S(a,b,q) defined by

$$F(a,b,q) = \iint d_3k\, d_3k'\, \delta\left(|k|^2-a^2\right) \delta\left(|k'|^2-b^2\right) \delta_3(k-k'-q) , \tag{8.2}$$

$$S(a,b,q) = \frac{b}{\pi a h^2 v v'} \iint dr\, dr'\, \exp[iq \cdot (r-r')]$$

$$\Sigma_f \langle K(r') \rangle_{of} \langle K(r) \rangle_{fo} \delta(E_f-E_o-E+E') . \tag{8.3}$$

Both F and S are evidently positive. Therefore we may obtain upper bounds to (8.1) by replacing F(a,b,q) by anything larger.

The integrations in (8.2) are easy to do, and are left as an exercise to the reader. The result is

$$F(a,b,q) = \frac{\pi}{2|q|} \tag{8.4}$$

if the triangle inequalities

$$|a-b| < |q| < a+b \tag{8.5}$$

are satisfied, and otherwise

$$F(a,b,q) = 0 \ . \tag{8.6}$$

Therefore we may insert (8.4) in (8.1) with the q-integration extended over the sphere

$$|q| < 2a \ . \tag{8.7}$$

Now by (7.16),

$$\frac{b}{v'} = \frac{E'}{\hbar c^2} \leq \frac{E}{\hbar c^2} = \frac{a}{v} \ . \tag{8.8}$$

Note that we used here the inequality (7.14) which forbids exothermic processes. When we use (8.8) to replace (b/v') by (a/v) in (8.3), S(a,b,q) is no longer dependent on E' except for the δ-function factor. After this replacement, the integration over E' in (8.1) becomes trivial and the δ-function in (8.3) disappears. The sum

over final states in (8.3) can then be performed by using the sum-rule

$$\Sigma_f \langle K(r') \rangle_{of} \langle K(r) \rangle_{fo} = \langle K(r') K(r) \rangle_{oo}. \tag{8.9}$$

After these manipulations, (8.1) implies

$$Av_\Omega \sigma_A(k) \leq \frac{1}{2ah^2v^2} \int d_3q \iint dr\, dr'$$

$$\exp[iq \cdot (r-r')] A(r',r), \tag{8.10}$$

where $A(r',r)$ is the autocorrelation function (7.10).

We now make use of the decomposition (7.11) and the bounds (7.12), (7.13). In the part of (8.10) involving $B(r',r)$, we extend the q-integration to infinity and use the identity

$$\int d_3q \exp [iq \cdot (r-r')] = (2\pi)^3 \delta(r-r') . \tag{8.11}$$

In the part involving $S(r',r)$, we use the inequality

$$\left| \int d_3q \exp[iq \cdot (r-r')] \right| \leq \frac{32\pi a^3}{3} , \tag{8.12}$$

the right side being the volume of the sphere (8.7). We thus obtain from (8.10), (7.12) and (7.13)

$$\mathrm{Av}_{\Omega}\ \sigma_A(k) \leq \left(\frac{G^2a^2}{h^2v^2}\right)\left[\frac{1}{2}\lambda^3\int\rho^2dr + \frac{16\pi}{3}\int\rho dr\right] . \tag{8.13}$$

Here

$$\lambda = 2\pi a^{-1} \tag{8.14}$$

is the wave-length of the incident neutrino, and

$$E = \hbar c^2(a/v) \tag{8.15}$$

is its energy. Furthermore

$$V = \int dr \tag{8.16}$$

is the volume of the scatterer, and

$$N = \rho V \tag{8.17}$$

is the number of particles contained in it. Thus (8.13) becomes

$$\mathrm{Av}_{\Omega}\sigma_A(k) \leq N\left(\frac{G^2E^2}{\hbar^4c^4}\right)\left[\frac{4}{3\pi} + \frac{1}{8\pi^2}\rho\lambda^3\right] . \tag{8.18}$$

We have proved Theorem 1, with σ_1 equal to a sum of two terms

$$\sigma_1 = \sigma_i + \sigma_c \rho\lambda^3. \tag{8.19}$$

The two parts of the cross-section σ_1 correspond exactly to our physical expectations for the incoherent and coherent scattering of neutrinos by an assemblage of particles with density ρ. The first part is just a typical cross-section for the scattering of neutrinos by a single particle. Multiplied by N, it gives the incoherent scattering by N particles. The second part in (8.19) is the cross-section for coherent scattering by particles within a volume of order λ^3. Multiplied by N, it gives the cross-section for coherent scattering by N particles. Two particles can contribute coherently to the angle-averaged cross-section only when they are within a neutrino wavelength from one another.

8.2 Proof of Theorem 2

When we substitute (7.15) into (7.18) and average over energy according to (6.8), the result is

$$\mathrm{Av}_E\, \sigma_B(k) = \iint d_3q\, d\Delta\, R(q,\Delta)\, S(q,\Delta)\ , \tag{8.20}$$

with the factors $R(q,\Delta)$ and $S(q,\Delta)$ defined by

$$R(q,\Delta) = \Sigma_f \, \delta(E_f - E_o - \Delta) \iint dr \, dr'$$

$$\exp\{iq \cdot (r-r')\} < (K(r') >_{of} < K(r) >_{fo}, \qquad (8.21)$$

$$S(q,\Delta) = \frac{1}{4\pi^2\hbar} \int_o^1 dx \, (\frac{1}{v}) \, (1 - \frac{v'}{v} \cos\theta) \, \delta(xE - E' - \Delta) \, . \qquad (8.22)$$

In (8.22) the energy E' is implicitly a function of x, since

$$E' = \left(M'^2c^4 + \hbar^2c^2(k-q)^2\right)^{1/2} \qquad (8.23)$$

with k defined by

$$xE = (M^2c^4 + \hbar^2c^2k^2)^{1/2} \, . \qquad (8.24)$$

The definition (6.8) of energy-averaging implies that the incident wave-vector k keeps its direction fixed while its magnitude varies with x according to (8.24). Differentiation of (8.23) and (8.24) then gives

$$dE' = \hbar v' \cos\theta \, dk, \; Edx = \hbar v dk \, , \qquad (8.25)$$

and therefore

$$\frac{dE'}{dx} = E\left(\frac{v'}{v}\right) \cos\theta \ , \tag{8.26}$$

$$\frac{d}{dx}\left(xE - E' - \Delta\right) = E\left(1 - \frac{v'}{v}\cos\theta\right) . \tag{8.27}$$

The integration over the delta-function in (8.22) thus precisely cancels the factor $\left(1 - (v'/v)\cos\theta\right)$ in the integrand. The result of the integration is

$$S(q,\Delta) = \frac{1}{4\pi^2 \hbar v E} \tag{8.28}$$

if the equation

$$xE - E' - \Delta = 0 \tag{8.29}$$

has a solution between $x = 0$ and $x = 1$, and zero otherwise. There cannot be more than one solution since the derivative (8.27) is positive. We now use the fact that for a neutrino $v = c$, so that

$$S(q,\Delta) \leq \frac{1}{4\pi^2 \hbar c E} \ , \tag{8.30}$$

the bound being independent of q and Δ. When (8.30) is substituted into (8.20), the integration over Δ is trivial and the sum over final states can be performed using (8.9) as before. The result is

$$Av_E\ \sigma_B(k) \leq \frac{1}{4\pi^2 \hbar c E} \int d_3q \iint dr\ dr' \exp\,[iq \cdot (r-r')]\ A(r',r)\ . \tag{8.31}$$

The bound here is identical with (8.10) apart from a factor of 2, and the proof of Theorem 2 from this point on is the same as the proof of Theorem 1.

8.3 Proof of Theorem 3

Let u be a unit vector pointing in an arbitrary direction. For any other vector such as v, we denote by $v_\parallel$ the component of v parallel to u, and by $v_\perp$ the component of v perpendicular to u. We shall study the weighted cross-section

$$\sigma_u(k) = \iint \sigma\ (k,k') \left|\frac{v'_\perp}{v}\right| d\Omega'\ dE'\ . \tag{8.32}$$

When $\sigma_u(k)$ is averaged over all directions of u, the result is according to (7.20)

$$Av_u\ \sigma_u(k) = \frac{1}{2}\ \sigma_v(k)\ . \tag{8.33}$$

We substitute from (7.15) into (8.32) and obtain

$$\sigma_u(k) = \frac{1}{4\pi^2\hbar v^2} \int d_3q \int d\Delta\ |v'_{\parallel}|$$

$$\delta(E-E'-\Delta)\ R(q,\Delta)\ , \tag{8.34}$$

with $R(q,\Delta)$ again given by (8.21). We now divide the q integration into integrations over $q_{\parallel}$ and $q_{\perp}$ separately. The integration over $q_{\parallel}$ is done first, holding E, Δ and $q_{\perp}$ fixed. We have then

$$\frac{dE'}{dq_{\parallel}} = \frac{\hbar^2c^2(k-q)_{\parallel}}{E'} = \hbar v'_{\parallel}. \tag{8.35}$$

The integration over the delta-function in (8.34) then just cancels the factor $|v'_{\parallel}|$. We find

$$\int dq_{\parallel}\ \hbar|v'_{\parallel}|\ \delta(E-E'-\Delta) \leq 2\ , \tag{8.36}$$

since the equation

$$E - E' - \Delta = 0 \tag{8.37}$$

holds for at most two values of $q_\parallel$. Therefore (8.34) implies

$$\sigma_u(k) \leq \frac{2}{h^2v^2} \iint d_2q_\perp d\Delta R(q,\Delta) \ . \tag{8.38}$$

The integration over Δ is (8.21) can now be done trivially, and the sum over final states f is done using (8.9). Then (8.38) becomes

$$\sigma_u(k) \leq \frac{2}{h^2v^2} \int d_2q_\perp \iint dr\ dr'$$

$$\exp[iq \cdot (r-r')]\ A(r',r) \ . \tag{8.39}$$

The parallel component $q_\parallel$ still appears in (8.39), being defined implicitly by the equation (8.37). But since the whole expression (8.21) is positive definite, the inequality remains valid if we replace the complex phase-factor

$$\exp[iq_\parallel(r-r')_\parallel] \tag{8.40}$$

by unity.

We now divide A(r',r) into its two parts according to (7.11), and estimate the two parts separately as we did in dealing with

(8.10). We have instead of (8.11)

$$\int d_2 q_\perp \exp\,[iq_\perp \cdot (r-r')] = (2\pi)^2\, \delta(r-r')_\perp\,, \tag{8.41}$$

and instead of (8.12), since $q_\perp$ now lies within a circle of radius a,

$$\left| \int d_2 q_\perp \exp[iq_\perp \cdot (r-r')] \right| \leq \pi a^2. \tag{8.42}$$

After these maneuvers, (8.39) with (7.12) and (7.13) implies

$$\sigma_u(k) \leq \left(\frac{G^2E^2}{\hbar^4 c^4}\right) \left[\frac{\lambda^2}{2\pi^2} \iint \rho^2\, \delta_2(r-r')_\perp \, dr\, dr' \right.$$

$$\left. + \frac{1}{2\pi} \int \rho dr \right]. \tag{8.43}$$

It remains only to average over the direction u. A simple calculation gives

$$\mathrm{Av}_u[\delta_2(r-r')_\perp] = \frac{1}{2\pi |r-r'|^2}\,. \tag{8.44}$$

Therefore (8.33) and (8.46) give

$$\sigma_v(k) \leq \left(\frac{G^2E^2}{\hbar^4 c^4}\right) \left[\frac{\lambda^2}{2\pi^3} \iint \rho^2 \frac{dr\, dr'}{|r-r'|^2} + \frac{1}{\pi} \int \rho dr \right]. \tag{8.45}$$

The integral

$$\iint \frac{dr\, dr'}{|r-r'|^2} \tag{8.46}$$

extended over the volume of the scatterer is equal to

$$S\, V^{4/3}, \tag{8.47}$$

where V is the volume of the scatterer and S is a numerical factor depending on its shape. So finally (8.45) with (8.16) and (8.17) implies

$$\sigma_v(k) \leq \left(\frac{G^2E^2}{\hbar^4 c^4}\right) \left[\frac{S}{2\pi^3} (\rho\lambda^3)^{2/3} N^{4/3} + \frac{1}{\pi} N\right] . \tag{8.48}$$

This completes the proof of Theorem 3. The division of the bound (8.48) into coherent and incoherent contributions occurs exactly as in the case of Theorem 1. As should be expected on physical grounds, only the coherent contribution is proportional to $N^{4/3}$.

8.4 Proof of Theorem 4

The proof of Theorem 4 follows the same lines as the proof of Theorem 3. The only change is that the factor $(1-(E'/E))$ appears in (7.21). This factor will then appear as an additional factor

$$\frac{\Delta}{E} = \frac{E_f - E_o}{E} \tag{8.49}$$

in (8.34) and in the definition (8.21) of $R(q,\Delta)$. Now we can absorb this factor into the matrix elements in (8.21) by using the identity

$$(E_f - E_o) < K(r) >_{fo} = < L(r) >_{fo}, \tag{8.50}$$

where L(r) is the commutator

$$L(r) = [H, K(r)] \tag{8.51}$$

and H is the Hamiltonian operator of the scatterer. L(r) will be a local current operator like K(r).

As in the proof of Theorem 3, we introduce instead of (8.32)

$$\sigma'_u(k) = \iint \sigma(k,k') \left(1 - \frac{E'}{E}\right) \left|\frac{v'}{v}\right|_\perp d\Omega' \, dE' \qquad (8.52)$$

so that

$$Av_u \, \sigma_u'(k) = \frac{1}{2} \sigma_w(k). \qquad (8.53)$$

Then we obtain instead of (8.39)

$$\sigma'_u(k) \leq \frac{2}{h^2 v^2 E} \int d_2 q_\perp \iint dr \, dr'$$

$$\exp\,[iq \cdot (r-r')] \, A'(r',r) \, , \qquad (8.54)$$

with

$$A'(r',r) = \langle K(r') \, L(r) \rangle_{oo} \qquad (8.55)$$

instead of (7.10). We might now go on to separate $A'(r', r)$ into two parts, one bounded and one short-range, as in (7.11). But this is unnecessary. Since q is only an integration-variable, the value of (8.54) is unchanged when we replace q by (-q). Since q, r and r' are coupled only in the exponential phase-factor, the value of (8.54) is still unchanged when we change (-q) back to q and interchange r and r'. Therefore (8.54) remains true if we use the definition

$$A'(r',r) = \frac{1}{2} < K(r')\ L(r) + K(r)\ L(r') >_{oo} \qquad (8.56)$$

for $A'(r',r)$ instead of (8.55). But the definition (8.51) of $L(r)$ enables us to write the operator on the right of (8.56) as a sum of three commutators

$$K(r')\ L(r) + K(r)\ L(r') = \frac{1}{2}\,[H,\{K(r')\ K(r) + K(r)\ K(r')\}]$$

$$- \frac{1}{2}\,[L(r),\ K(r')] - \frac{1}{2}[L(r'),\ K(r)]\ . \qquad (8.57)$$

The first commutator contributes nothing to the expectation value, and therefore

$$A'(r',r) = -\frac{1}{4} < [L(r),\ K(r')] + [L(r'),\ K(r)] >_{oo}. \qquad (8.58)$$

Now $L(r)$ and $K(r')$ are both local currents, and so their commutator is zero for $r \neq r'$. In fact the commutators in (8.58) are not merely short-range, they are zero-range in $(r-r')$. Thus $A'(r',r)$ is a local current-density at r multiplied by a delta-function or a derivative of a delta-function of $(r-r')$. The long-range part of $A'(r',r)$ is absent.

The proof of Theorem 4 proceeds from this point onward like the proof of Theorem 3, but with the long-range coherent term absent on the right side of (8.43), (8.45) and (8.48). At the end we obtain instead of (8.48)

$$\sigma_W(k) \leq Nf \frac{G^2E^2}{\hbar^4 c^4} , \tag{8.59}$$

where f is a numerical factor depending on the local behavior of the operators L(r) and K(r). Since the definitions (7.20), (7.21) imply

$$\sigma_W(k) \leq \sigma_V(k) , \tag{8.60}$$

the incoherent part of $\sigma_V(k)$ will be an upper bound for $\sigma_W(k)$, and therefore (8.59) holds with $f = (1/\pi)$. This completes the proof of Theorem 4.

DISTRIBUTION LIST

Dr. Marv Atkins [3]
Deputy Director, Science & Tech.
Defense Nuclear Agency
Washington, D.C. 20305

LTCOL Joseph Bailey
Office of Science & Technology Policy
Room 5026
New Excutive Office Bldg
17th & Pennyslvania
Washington, DC 20506

Dr. Art Bisson
Technical Director of Submarine and SSBN Security Program
Department of the Navy
OP-02T
The Pentagon, Room 4D534
Washington, DC 20350-2000

Dr. Curtis G. Callan
Princeton University
Princeton, NJ

Dr. Raymond Collady
Director
DARPA
1400 Wilson Boulevard
Arlington, VA 22209

Dr. Ron Clark
DARPA/NTO
1400 Wilson Blvd.
Arlington, VA 22209

Mr. John Darrah
Sr. Scientist and Technical Advisor
HQ Space Cmd/XPN
Peterson AFB, CO 80914

Defense Technical Information [2] Center
Cameron Station
Alexandria, VA 22314

RADM Craig E. Dorman
Director, ASW Programs
Code PD-80
Department of the Navy
Washington, D.C. 20363-5100

Dr. Freeman J. Dyson
Institute for Advanced Study
Princeton, NJ

Mr. John Entzminger
DARPA
1400 Wilson Blvd.
Arlington, VA 22209

Mr. Robert Foord [2]
P.O. Box 1925
Washington, D.C. 20505

Dr. Larry Gershwin
NIO for Strategic Programs
P.O. Box 1925
Washington, D.C. 20505

The Honorable Richard P. Godwin
Under Secretary for Defense of Acquisition
The Pentagon, Room 3E1006
Washington, D.C. 20301

Dr. S. William Gouse, Z605
Senior Vice President and General Manager
The MITRE Corporation, Metrek Division
7525 Colshire Drive
McLean, VA 22102

Dr. Mario Grossi
Raytheon Company
Submarine Signal Division
P.O. Box 360
1847 W. Main Road
Portsmouth, RI 02871

Mr. Jack Hammond
Strategic Defense Initiative
Organization
1717 H. Street
Washington, D.C. 20301

Dr. William Happer
Princeton University
Princeton, NJ 08540

Dr. Robert G. Henderson
Director, JASON Program Office
The MITRE Corporation
7525 Colshire Drive
McLean, VA 22102-3481

Mr. R. Evan Hineman
Deputy Director for Science
& Technology
Central Intelligence Agency
Washington, D.C 20505

CDR Earl R. Jones
NAVOPINTCEN
Attn: 06 Dept
4301 Suitland Road
Suitland, MD 20390-5170

Mr. Edwin L. Key
Senior Vice President
for Research and Engineering
The MITRE Corporation
P.O. Box 208
Bedford, MA 01730

MAJGEN Donald L. Lamberson
Assistant Military Deputy for
Acquisition
(RD&A) HQ USAF/RD, Rm. 4E334
Washington, D.C. 20330-5010

MAJ George P. Lasché
DARPA
1400 Wilson Boulevard
Arlington, VA 22209

The MITRE Corporation [5]
7525 Colshire Drive
McLean, VA 22102
ATTN: JASON Library, W002

Dr. Gordon MacDonald, Z605
Vice President
and Chief Scientist
The MITRE Corporation
7525 Colshire Drive
McLean, VA 22102

Director [2]
National Security Agency
Department of Defense
Fort Meade, MD 20755
ATTN: Mr. Richard Madden, R9

Mr. Charles Mandelbaum
Mail Stop ER-32/G-226 GTN
U.S. Department of Energy
Washington, D.C. 20545

Dr. Allan T. Mense
Strategic Defense Initiative
Organization
The Pentagon, Room 3C444
Washington, D.C. 20301

Mr. Mewson
HQ SAC/NRI
Offutt AFB
Nebraska 68113-5001

Dr. Julian Nall [2]
NIO/S&T
Central Intelligence Agency
Washington, D.C. 20505

Superintendent (Code 1424)
Naval Postgraduate School
Monterey, CA 93943
Attn: Documents Librarian

Director
National Security Agency
Fort Meade, MD 20755
ATTN: Mr. Edward P. Neuburg
DDR-FANX III

Dr. Robert L. Norwood [2]
Acting Director for Space
Office of the Assistant Secretary
of the Army
(Research, Development & Acq)
The Pentagon, Room 2E673
Washington, D.C. 20310-0103

BG Malcolm O'Neil
Strategic Defense Initiative
Organization
The Pentagon
Washington, DC 20310-0103

Dr. Francis W. Perkins, Jr.
Princeton University
Princeton, NJ

Major Donald R. Ponikvar
Department of the Army
Strategic Defense Command
P. O. Box 15280
Arlington, VA 22215-0150

Mr. John Rausch
NAVOPINTCEN Detachment, Suitland
4301 Suitland Road
Washington, D.C. 20390

The MITRE Corporation
Records Resources
Mail Stop W971
McLean, VA 22102

Dr. Richard Reynolds
DARPA
1400 Wilson Blvd.
Arlington, VA 22209

Mr. Alan J. Roberts, Z605
Senior Vice President
Washington C^3I Operations
The MITRE Corporation
7525 Colshire Drive
McLean, VA 22102

Mr. Thomas Rona
Deputy Director
Office of Science & Tech
Policy
Old Executive Office Bldg
17th & Pennsylvania Ave., N.W.
Washington, D.C. 20500

Dr. Fred Saalfeld
Technical Director
Office of Naval Research
800 N. Quincy Street
Arlington, VA 22217

Dr. Phil Selwyn [2]
Technical Director
Office of Naval Technology
800 N. Quincy Street
Arlington, VA 22217

DISTRIBUTION LIST (Cont'd.)

Mr. Shen Shey
DARPA
1400 Wilson Blvd.
Arlington, VA 22209

Dr. Gordon Smith
Strategic Defense Initiative
Organization
The Pentagon
Washington, D.C. 20301

Dr. Joel A. Snow [2]
Director
Science & Tech. Staff
U.S. DOE/ER-6
Washington, D.C. 20585

COMO William O. Studeman
Director of Naval Intelligence
Office of Naval Intelligence
Navy Department (OP-009)
Washington, D.C. 20310

Mr. Alexander J. Tachmindji, Z605
Senior Vice President
The MITRE Corporation
7525 Colshire Drive
McLean, VA 22102

Dr. Vigdor Teplitz
National Science Foundation
7008 Winslow Street
Bethesda, MD 20817

Dr. Sam B. Treiman
Princeton University
Princeton, NJ

Professor Joseph Weber
Genral Relativity
Department of Physics and
Astronomy
University of Maryland
College Park, MD 20742

Mr. Charles A. Zraket
President
The MITRE Corporation
P.O. Box 208
Bedford, MA 01730